Geology

Magnetic and geochemical characteristics of Gobi Desert surface sediments: Implications for provenance of the Chinese Loess Plateau

Barbara A. Maher, Thomas J. Mutch and Dickson Cunningham

Geology 2009;37;279-282
doi:10.1130/G25293A.1

Notes

Magnetic and geochemical characteristics of Gobi Desert surface sediments: Implications for provenance of the Chinese Loess Plateau

Barbara A. Maher[1]*, Thomas J. Mutch[1], Dickson Cunningham[2]
[1]Centre for Environmental Magnetism and Palaeomagnetism, Lancaster Environment Centre, University of Lancaster, Lancaster LA1 4YQ, UK
[2]Department of Geology, University of Leicester, University Road, Leicester LE1 7RH, UK

ABSTRACT

Controversy exists regarding the sources of the eolian dust for the immense Loess Plateau of north-central China, the largest accumulation of windblown loess in the world. Because the loess accumulation rate, unit thickness, and particle size all decrease from northwest to southeast, it has long been thought that the northern deserts, especially the Mongolian Gobi, are the major loess source, a view supported by newly applied mineralogical provenance techniques (electron spin resonance, ESR). Here, we examine surface samples from the Gobi Desert and compare their magnetic and geochemical properties with those of last glacial loess samples from across the Loess Plateau region. The mineralogy, geochemistry, and magnetic properties of Gobi Desert samples are variable (most likely reflecting local lithological complexity), distinctive, and, critically, nonoverlapping with the notably homogenous characteristics of the last glacial loesses spanning the Loess Plateau. It is likely that the source areas for the plateau encompass a much larger area than any one proximal desert region, in order to account for (1) the extreme degree of mixing, (2) the volume of loess generated and transported, and (3) the mineralogical and magnetic mismatch evident here between the Mongolian Gobi samples and the last glacial loess.

INTRODUCTION

The famous Loess Plateau of north-central China comprises an immense wedge of eolian-derived sediment (~2 × 10^5 km^3 in volume) extending over ~4.4 × 10^5 km^2, from the southern margin of Mongolia and eastern margin of Tibet to the middle reaches of the Huáng Hé, and thence south and east to Xi'an and Beijing (Fig. 1). The loess is thickest in the northwest (>~300 m), thinning to ~150 m in the central and southern plateau areas. This body of quasi-continuously deposited sediment represents a key Quaternary paleoclimatic archive, the most complete terrestrial record of climatic and environmental change through the Quaternary and earlier (e.g., Liu, 1988; Wang et al., 2005). The sequences document the evolution and ongoing variability of atmospheric circulation and continental paleoclimate (especially the East Asian summer and winter monsoon systems), as recorded by variations in their magnetic properties (e.g., Maher and Thompson, 1992, 1999; Heller and Evans, 1995; Maher, 2008), particle size (e.g., Prins et al., 2007), carbonate content, and isotopic composition (e.g., Rowe and Maher, 2000; Honda et al., 2004; Chen et al., 2006).

To generate and displace loess on this scale, efficient formation and transport of silt- and finer-sized particles has occurred over the last ~2.5 m.y. or more. For the Chinese Loess Plateau, possible source areas for this volume of rock breakdown and dust generation encompass arid and semiarid areas of the northern and northwestern deserts (Fig. 1), including the Gobi (Inner Mongolia), Mu Us, Qaidam Basin, Junggar, Ordos, and Tengger. Significantly more distant to the west lies the Taklimakan Desert, the most extensive sand desert in China (~3.5 × 10^3 km^2), with a high frequency of severe dust storm activity (>50 d/yr; Pye and Zhou, 1989). Additionally, fine-particle generation by cold-climate processes (periglacial and glacial rock fracture) continues in the uplifting Tibetan and Himalayan regions. However, the loess thickness, accumulation rate, and particle size all decrease from the northwest to the southeast of the Loess Plateau, the basis for the traditional view that the northern deserts, especially the Gobi, have been the major loess source (e.g., An, 2000). This view is consistent with the pattern of wind flows at the last glacial maximum, when northwesterly/westerly surface winds predominated during the winter monsoon (Fig. DR1 in the GSA Data Repository[1]). In geochemical terms, north-to-south decreases in the zirconium/rubidium ratio have been reported for the last glacial loess units of the plateau, with little west-east variation (Chen et al., 2006). Most recently, Sun et al. (2008) have used electron spin resonance (ESR) and the crystallinity of fine quartz particles to identify loess sources through past climate stages. In line with the conventional view, they find that the far-traveled dust derived mainly

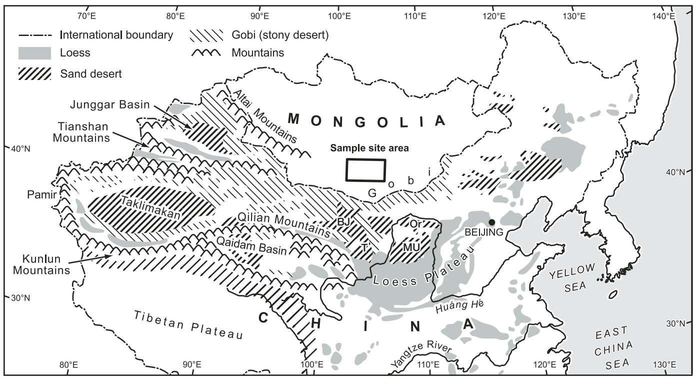

Figure 1. Map showing the spatial extent of the Chinese Loess Plateau and surrounding potential desert source areas. Or—Ordos; BJ—Badain Juran; T—Tengger; Mu—Mu Us.

*E-mail: b.maher@lancaster.ac.uk.

[1]GSA Data Repository item 2009070, Figures DR1–DR3 and Tables DR1 and DR2, is available online at www.geosociety.org/pubs/ft2009.htm, or on request from editing@geosociety.org or Documents Secretary, GSA, P.O. Box 9140, Boulder, CO 80301, USA.

from the Gobi Desert and two sandy deserts in northern China (the Badain Juran and Tengger Deserts), at least during the last climatic cycle.

Here, we present paired magnetic and geochemical data for surface samples from the Gobi Desert, to examine the suggested affinity between the Gobi and the last glacial loess. The distinctive characteristics of the Gobi surface samples provide a timely opportunity to examine the view, long-standing and current, that this area has been a major dust source for the Loess Plateau during past glacial stages.

METHODS

Eighteen surface samples were obtained from an area spanning ~12,000 km^2 in central and northern areas of the Gobi Desert in Mongolia (102°17′E to 105°25′E, 43°42′N to 44°31′N; Fig. 1); the majority are alluvial fan sediments, and the westernmost samples are from a major longitudinal dune field. All sample sites lie within areas open to deflation, either broad low areas in the north and northeast or topographic corridors that funnel wind down their axes (Fig. DR2). For particle size analysis, organic matter was removed from the bulk fanglomerate samples, which were sequentially sieved to retain the sand- and finer-sized fractions, and then ultrasonically dispersed and analyzed using a laser diffraction particle analyzer (see Appendix). To obtain particle sizes most representative of material deflated and transported by the wind, dispersed samples were split by wet sieving into 38–63 μm and <38 μm size fractions. Magnetic measurements, on each size fraction, included low-field, initial magnetic susceptibility; susceptibility of anhysteretic remanence (χ_{ARM}; i.e., the ARM normalized by the DC bias field); and stepwise acquisition and AC demagnetization of isothermal (room temperature) remanent magnetization (IRM). X-ray powder diffraction (XRPD) was undertaken on both size fractions to identify major and minor mineral constituents. For comparability with the loess units of the plateau (dominated by silt-sized particles), the finer, <38 μm sample fractions were subjected to X-ray fluorescence (XRF) analyses, to identify their major and minor elemental concentrations.

RESULTS

The particle size distribution of potential source materials is important. Most dust particles transported by the atmosphere are <50 μm in diameter, yet >90% of particles present in most Chinese deserts exceed this size (e.g., Tsoar and Pye, 1987). Only three desert areas have been reported with significantly finer particle size distributions: the Gobi of the western Inner Mongolia Plateau, the Gobi of the central Inner Mongolia Plateau, and the western Taklimakan (e.g., Wang et al., 2004). The Gobi surface samples display a broad range of particle size distributions (Fig. DR3), but the majority contain significant proportions of fine, wind-transportable particles. The proportion of particles <50 μm varies from 2 to 45 vol%, with a mean value of 25 vol%. Particle size end members have been identified for the Loess Plateau sediments (Prins et al., 2007). These end members comprise a "sandy loess" component (modal particle size = 63 μm), a "silty loess" mode at 37 μm, and a "clayey loess" mode at 22 μm. The two coarser end members are thought to reflect saltation and suspension of "local" coarse dust during dust storms in spring, and the finer end member to reflect higher-level transport by background and dust storm supply. The Gobi surface samples contain 28 vol% sandy loess, 18 vol% silty loess, and 16 vol% clayey loess.

The Gobi samples comprise quartz as their major mineral constituent ($\bar{x}$ = 52 wt% in the coarse fractions; $\bar{x}$ = 42 wt % in the fine fractions), followed by Na-plagioclase ($\bar{x}$ = 9 wt % in the coarse fractions; $\bar{x}$ = 8 wt % in the fine fractions) and calcite ($\bar{x}$ = 6 wt % in the coarse fractions; $\bar{x}$ = 12 wt % in the fine fractions). Significant proportions (i.e., >50 wt %) of the plagioclase occur as albite. A diverse range of other minerals occurs as minor (<~5 wt %) and variable constituents, including dolomite, clay minerals (chlorite, muscovite, illite), tremolite, zoisite, garnet, tourmaline, zircon, barite, goethite, hematite, and iron/titanium oxides (Table DR1).

Table DR1 also summarizes the magnetic properties of the Gobi surface samples for the 38–63 μm and <38 μm particle size fractions. The magnetic properties of most natural samples reflect the presence of trace amounts of strongly magnetic magnetite and maghemite, and minor amounts of weakly magnetic hematite and goethite. For samples devoid of these minerals, magnetic susceptibility can be low and positive (arising from paramagnets such as clay minerals) or low and negative (from diamagnets such as quartz). The magnetic data indicate that the Gobi samples contain a mixture of magnetic grain sizes and minerals, including magnetite-like grains dominantly of 1 μm or larger (Maher, 1988) and significant proportions of the weaker magnetic minerals, hematite and/or goethite. Magnetic susceptibility values for the coarse Gobi fractions range from 32 to 322 × 10^{-8} m^3 kg^{-1} (n = 18, $\bar{x}$ = 170, σ = 74 × 10^{-8} m^3 kg^{-1}), and for the fine fractions range from 47 to 295 × 10^{-8} m^3 kg^{-1} (n = 18, $\bar{x}$ = 111, σ = 52 × 10^{-8} m^3 kg^{-1}). These mean values indicate magnetite concentrations of between 0.6 and 0.2 wt %, respectively. In contrast, the susceptibility of unweathered loess, i.e., in the arid western Loess Plateau (e.g., Maher and Thompson, 1999; Jeong et al., 2008), or of loess treated in the laboratory to remove any in situ pedogenic magnetite (Hunt et al., 1995), is consistently ~20–30 × 10^{-8} m^3 kg^{-1}, indicating a detrital (lithogenic) magnetite concentration of <0.05 wt %.

The major (wt%) and trace element (ppm) compositions of the Gobi samples (<38 μm) are available from Table DR2. Figures 2A and 2B show selected major element abundances for the Gobi, and for loess units (L_1 and L_2) from the last two glacial stages, from sites spanning the

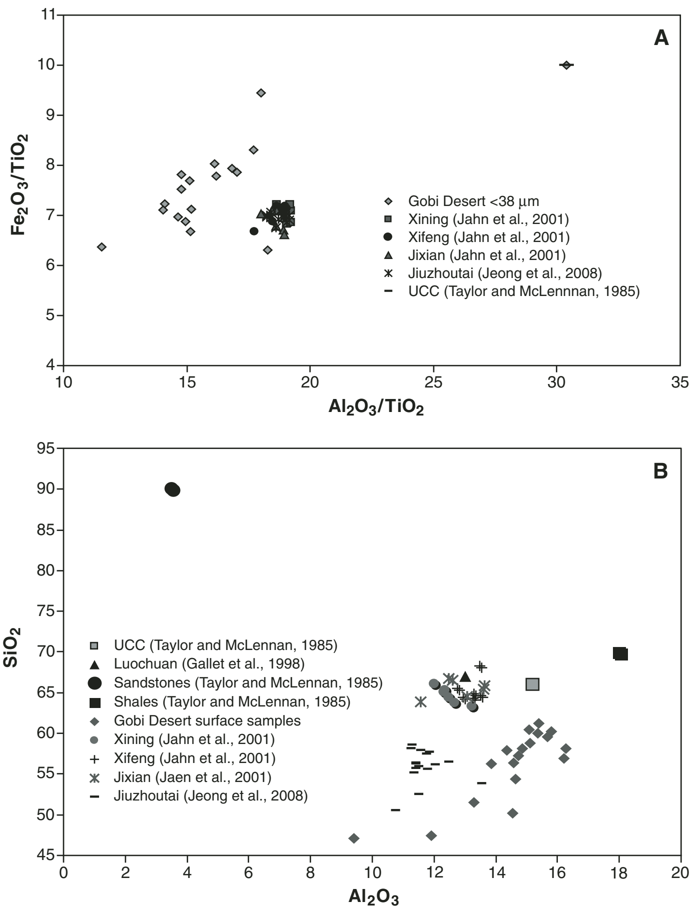

Figure 2. Major element ratios and abundances for the Gobi surface samples (<38 μm) and for last glacial loess units from across the Chinese Loess Plateau. A: Fe_2O_3/TiO_2 versus Al_2O_3/TiO_2. B: SiO_2 versus Al_2O_3. UCC—upper continental crust.

present-day rainfall gradient across the plateau. The Gobi samples have lower Al_2O_3/TiO_2 and higher Fe_2O_3/TiO_2 ratios than the loess units, which cluster tightly irrespective of their location (Fig. 2A). Similar Gobi/loess disparity is evident in their SiO_2 and Al_2O_3 components (Fig. 2B). Figure 3 combines the magnetic susceptibility and Fe_2O_3/Al_2O_3 data for the Gobi and glacial loess samples. The Gobi samples show scatter but display higher magnetic susceptibility and Fe_2O_3/Al_2O_3 ratios than the loesses.

DISCUSSION

The distinctive mineralogy, geochemistry, and magnetic properties of these Gobi Desert samples provide a timely opportunity to test the view that the Mongolian Gobi has been a major source area for the Chinese Loess Plateau (e.g., Sun et al., 2008; An, 2000).

Here, the Gobi surface samples not only display more variation, but also display little if any overlap with a geographic range of last glacial Loess Plateau samples. The mineralogy of the Gobi samples indicates a broad range of lithological sources, reflecting the complex of terranes in this region (Badarch et al., 2002). The basement rocks of the Gobi Altai represent one of the most diverse terrane mosaics on Earth; thus, the eroded geology is also diverse. Surrounding the sample sites are terranes including the Gobi Altai (backarc-forearc basin), Mandalovoo and Gurvan Sayhan (island arcs), Zoolen (accretionary prism), and possibly the Idermeg (passive continental margin). The surface sample mineralogy matches well the local northeastern Gobi Altai geology, which has high contents of quartz (from granites, sandstones, metasediments), albite (the typical plagioclase phase in the greenschist-grade metavolcanics and metavolcaniclastic sediments abundant in the area, including green phyllites, slates, and psammites), and significant metamorphic and igneous silicate minerals, all common in basement rocks in the Gurvan Sayhan and surrounding ranges. Similarly, iron oxides and hydroxides are widespread in the region's Mesozoic rocks (typically red-bed clastic sediments). Magnetic susceptibility values for the surface samples are slightly higher in the 38–63 µm fractions, indicating predominantly lithogenic iron oxide grains. The presence of calcite and dolomite, in both the 38–63 µm and <38 µm size fractions, indicates they most likely originate from limestones, metamorphosed calcareous rocks, and/or evaporative deposits. Carbonate cements occur in the Mesozoic sediments, and caliche-rich horizons are common in the Cretaceous cover. Since the surface sample mineralogy is consistent with local/regional source rocks, the surface samples are probably not very far-traveled.

In terms of availability of wind-erodible material, the surface samples contain significant volumes of silt- and finer-sized particles; indeed, the western samples originate from an active longitudinal dune field, Hongorin Els ("singing sands"). Landsat imagery reveals wind streaking all over southern and western Mongolia, typically trending WNW-ESE consistent with the prevailing northwesterly surface winds. Most of the intramontane basins have well-developed desert pavement with ventifacts. Traynor and Sladen (1995) suggest that eolian deflation accounts for up to 50 wt % of the sediment removed from the Gobi Altai intramontane basins.

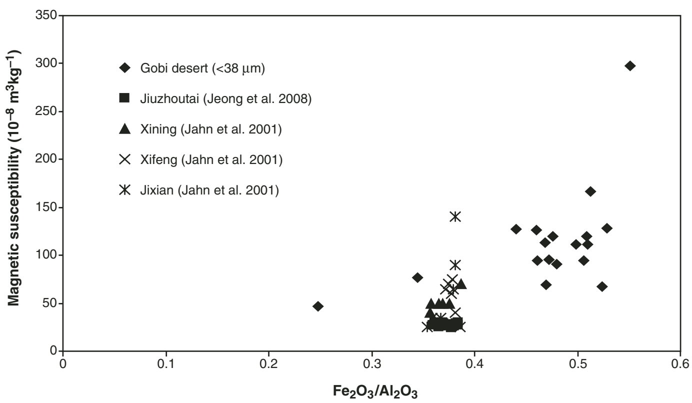

Figure 3. Magnetic susceptibility and Fe_2O_3/Al_2O_3 ratios for the Gobi surface samples (<38 µm) and for glacial loess units across the Loess Plateau.

Despite this eolian activity, the Gobi surface samples display striking disparity with the last glacial loesses from across the Chinese Loess Plateau. The Gobi samples are variably but more strongly magnetic, and have lower SiO_2 contents, higher Fe_2O_3/TiO_2 and lower Al_2O_3/TiO_2 ratios (see Figures 2A, 2B, and 3). These differences cannot be accounted for by particle size variations (e.g., resulting from wind winnowing) since these properties show no variation with particle size for the Gobi <38 µm size fractions. For the Gobi surface materials to have contributed significantly to the loess, admixing with and dilution by other, diamagnetic components (i.e., with negative magnetic susceptibility) would have been required on a major scale. For example, in order to produce the typical susceptibility of the unweathered loess, one part Gobi mean sample would need to be mixed with, e.g., ~80 parts calcium carbonate. The Gobi samples further differ from the loesses by dint of their heterogeneity. The loess samples, in contrast, are remarkably homogenous (e.g., Fig. 2A), despite spanning the west-east weathering/rainfall gradient across the Loess Plateau. These data indicate that the loess source materials have been extremely well mixed prior to deposition on the plateau, as noted by, e.g., Jahn et al. (2001) from uniform REE patterns and restricted Nd isotopic compositions.

Maher and Thompson (1999) have suggested that paired magnetic and ^{10}Be values might geologically constrain potential source areas; the loess displays variable but often very high ^{10}Be loadings (~0.5–5.5 × 10^8 atoms g^{-1}; e.g., Beer et al., 1993) and quite low magnetic susceptibility (~20–30 × 10^{-8} m^3 kg^{-1}). Given average ^{10}Be fluxes (Pavich et al., 1986), prolonged exposure (>1 m.y.) in a humid environment is required to account for the loess ^{10}Be loadings without incurring any weathering-derived increases in loess magnetic content. This combined high ^{10}Be and low magnetic content suggests a cold, humid source, such as the tectonically rising Himalayan/Tibetan regions. Thick beds of periglacial and/or glaciogenic silt occur on the Tibetan Plateau. Notable in this regard too are the southwesterly winter winds that blow from the Himalayas and Tibet toward the deserts to the north of the Loess Plateau (Fig. DR1). These southwesterly winds create a potential "dogleg" transport path for dust from the Tibetan/Himalayan regions to be blown first to the northern deserts, and thence, by springtime northwesterlies to the southeast, across the Loess Plateau. Tibetan and/or western desert sources have previously been suggested based on Nd/Sr isotopes (Honda et al., 2004) and compatible magnetic properties of Taklimakan Desert samples (Torii et al., 2001). It seems unlikely that any one desert area can be regarded as *the* major loess source; multiple, very large-scale source areas may have been tapped, with thorough mixing and possibly with recycling of materials during transport (possibly including transport and deposition processes along, e.g., the Yellow River). Multiple-proxy, rather than single-proxy, approaches appear to be a prerequisite for examining loess provenance, in order to avoid nonunique or spurious source identification. Application of such techniques to a wider geographic range of potential source areas is also a key future requirement.

CONCLUSIONS

The mineralogy, geochemistry, and magnetic properties of Gobi Desert samples are variable (most likely reflecting local lithological complexity) and distinctive, and, critically, they display little or no overlap with the notably homogenous characteristics of the last glacial loesses from across the Chinese Loess Plateau. It is likely that the source areas for the loess encompass a much larger area than any one proximal desert region, in order to account for the extreme degree of mixing of the loess, the very large volume of loess generated and transported, and the mineralogical and magnetic mismatch evident here between the Mongolian Gobi samples and glacial loess units across the Chinese Loess Plateau.

APPENDIX

For particle size analysis, samples were peroxidized to remove organic matter, ultrasonically dispersed in sodium hexametaphosphate, and analyzed using a laser diffraction particle analyzer (Coulter Counter Mastersizer).

Magnetic susceptibility was measured at 0.47 and 4.7 kHz using a Bartington MS2B susceptibility sensor. The ARM was imparted using a Molspin demagnetizer with ARM attachment at 80 millitesla (mT), with a 0.08 mT DC biasing field. IRM acquisition was incrementally imparted in DC fields of 20, 50, 100, and 300 mT (Molspin pulse magnetizer), and at 1 T (Newport electromagnet). All magnetic remanence measurements were made using a Molspin Minispin (noise level ~2.5×10^{-6} A m^2 kg^{-1}); all data are expressed on a mass-normalized basis.

XRPD analyses were made using a Philips PW170 diffractometer, with monochromatic Cu K_α radiation, 1° divergence slit and antiscatter slits, and a scan speed of 0.02° per step, counting for 2 s per step, over the range 3° to 60° 2θ. To produce unorientated slide mounts, samples were gently powdered, made into a slurry with acetone, and mounted evenly on a glass slide. Qualitative mineral analysis was made with reference to the JCPDS (Joint Committee on Powder Diffraction Standards, the International Centre for Diffraction Data) database; quantitative analysis was made using a peak modeling algorithm (Philips APD software). Major and minor elemental components were determined by XRF on high-dilution fused sample beads (0.1 g ignited sample to 3 g flux, lithium tetraborate) using a PANalytical Axios Advanced XRF spectrometer, at the Department of Geology, Leicester University. The fusion bead analysis, including determination of the loss on ignition (sample ignited at 1050 °C for 1 h and weight loss recorded), provides a normal lower limit of detection (LLD) of 0.01 wt %,with precision better than 0.5 wt % at 100 times the LLD. XRF calibration curves were established using 21 international and in-house reference standards.

ACKNOWLEDGMENTS

Maher received funding through a Royal Society–Wolfson Research Merit Award. Thanks are due to Nick Marsh, Leicester University, for the XRF analyses, and J. Chen and G.Y. Jeong, who kindly provided magnetic susceptibility data.

REFERENCES CITED

An, Z.S., 2000, The history and variability of the East Asian paleomonsoon climate: Quaternary Science Reviews, v. 19, p. 171–187, doi: 10.1016/S0277-3791(99)00060-8.

Badarch, G., Cunningham, W.D., and Windley, B.F., 2002, A new terrane subdivision for Mongolia: Implications for the Phanerozoic crustal growth of Central Asia: Journal of Asian Earth Sciences, v. 21, p. 87–110, doi: 10.1016/S1367-9120(02)00017-2.

Beer, J., Shen, C., Heller, F., Liu, T.S., Bonani, G., and Dittrich, B., 1993, ^{10}Be and magnetic susceptibility in Chinese loess: Geophysical Research Letters, v. 20, p. 57–60, doi: 10.1029/92GL02676.

Chen, J., Chen, Y., Liu, L.W., Ji, J.F., Balsam, W., Sun, Y.B., and Lu, H.Y., 2006, Zr/Rb ratio in the Chinese loess sequences and its implication for changes in the East Asian winter monsoon strength: Geochimica et Cosmochimica Acta, v. 70, p. 1471–1482, doi: 10.1016/j.gca.2005.11.029.

Gallet, S., Jahn, B.-M., and Torii, M., 1996, Geochemical characterization of the Luochuan loess-paleosol sequence, China, and paleoclimatic implications: Chemical Geology, v. 133, p. 67–88, doi: 10.1016/S0009-2541(96)00070-8.

Gallet, S., Jahn, B.-M., Van Vliet Lanoe, B., Dia, A., and Rossello, E., 1998, Loess geochemistry and its implications for particle origin and composition of the upper continental crust: Earth and Planetary Science Letters, v. 156, p. 157–172.

Heller, F., and Evans, M.E., 1995, Loess magnetism: Reviews of Geophysics, v. 33, p. 211–240, doi: 10.1029/95RG00579.

Honda, M., Yabuki, S., and Shimizu, H., 2004, Geochemical and isotopic studies of aeolian sediments in China: Sedimentology, v. 51, p. 211–230, doi: 10.1111/j.1365-3091.2004.00618.x.

Hunt, C.P., Singer, M.J., Kletetschka, G., TenPas, J., and Verosub, K.L., 1995, Effect of citrate-bicarbonate-dithionite treatment on fine-grained magnetite and maghemite: Earth and Planetary Science Letters, v. 130, p. 87–94, doi: 10.1016/0012-821X(94)00256-X.

Jahn, B.M., Gallet, S., and Han, J.M., 2001, Geochemistry of the Xining, Xifeng and Jixian sections, Loess Plateau of China: Eolian dust provenance and paleosol evolution during the last 140 ka: Chemical Geology, v. 178, p. 71–94, doi: 10.1016/S0009-2541(00)00430-7.

Jeong, G.Y., Hillier, S., and Kemp, R.A., 2008, Quantitative bulk and single-particle mineralogy of a thick Chinese loess-paleosol section: Implications for loess provenance and weathering: Quaternary Science Reviews, v. 27, p. 1271–1287.

Liu, T.-S., 1988, Loess in China: Berlin, Springer-Verlag, 224 p.

Maher, B.A., 1988, Magnetic properties of some synthetic sub-micron magnetites: Geophysical Journal of the Royal Astronomical Society, v. 94, p. 83–96.

Maher, B.A., 2008, Holocene variability of the East Asian summer monsoon from cave records: A re-assessment: The Holocene, v. 18, p. 867–876.

Maher, B.A., and Thompson, R., 1992, Paleoclimatic significance of the mineral magnetic record of the Chinese loess and paleosols: Quaternary Research, v. 37, p. 155–170, doi: 10.1016/0033-5894(92)90079-X.

Maher, B.A., and Thompson, R., 1999, Palaeomonsoons, I: The palaeoclimatic record of the Chinese loess and palaeosols, *in* Maher, B.A., and Thompson, R., eds., Quaternary climates, environments and magnetism: Cambridge, UK, Cambridge University Press, p. 81–125.

Pavich, M.J., Brown, L., Harden, J., Klein, J., and Middleton, R., 1986, ^{10}Be distribution in soils from Merced River terraces, California: Geochimica et Cosmochimica Acta, v. 50, p. 1727–1735, doi: 10.1016/0016-7037(86)90134-1.

Prins, M.A., Vriend, M., Nugteren, G., Vandenberghe, J., Lu, H.Y., Zheng, H.B., and Weltje, G.J., 2007, Late Quaternary aeolian dust input variability on the Chinese Loess Plateau: Inferences from unmixing of loess grain-size records: Quaternary Science Reviews, v. 26, p. 230–242, doi: 10.1016/j.quascirev.2006.07.002.

Pye, K., and Zhou, L.-P., 1989, Late Pleistocene and Holocene aeolian dust deposition in North China and the Northwest Pacific Ocean: Palaeogeography, Palaeoclimatology, Palaeoecology, v. 73, p. 11–23, doi: 10.1016/0031-0182(89)90041-2.

Rowe, P.J., and Maher, B.A., 2000, "Cold" stage formation of carbonate concretions in the Chinese loess and palaeosol sequences: Evidence from U-series dating and stable isotope analysis: Palaeogeography, Palaeoclimatology, Palaeoecology, v. 157, p. 109–126, doi: 10.1016/S0031-0182(99)00157-1.

Sun, Y., Tada, R., Chen, J., Liu, Q.S., Shin, T., Tani, A., Ji, J., and Yuko, I., 2008, Tracing the provenance of fine-grained dust deposited on the central Chinese Loess Plateau: Geophysical Research Letters, v. 35, L01804, doi: 10.1029/2007GL031672.

Taylor, S.R., and McLennan, S.M., 1985, The continental crust: Its composition and evolution: Boston, Blackwell Scientific, 312 p.

Torii, M., Lee, T.-Q., Fukuma, K., Mishima, T., Yamazaki, T., Oda, H., and Ishikawa, N., 2001, Mineral magnetic study of the Taklimakan desert sands and its relevance to the Chinese loess: Geophysical Journal International, v. 146, p. 416–424, doi: 10.1046/j.0956-540x.2001.01463.x.

Traynor, J.J., and Sladen, C., 1995, Tectonic and stratigraphic evolution of the Mongolian People's Republic and its influence on hydrocarbon geology and potential: Marine and Petroleum Geology, v. 12, p. 35–52, doi: 10.1016/0264-8172(95)90386-X.

Tsoar, H., and Pye, K., 1987, Dust transport and the question of desert loess formation: Sedimentology, v. 34, p. 139–153, doi: 10.1111/j.1365-3091.1987.tb00566.x.

Wang, X., Dong, Z., Zhang, J., and Liu, L., 2004, Modern dust storms in China: An overview: Journal of Arid Environments, v. 58, p. 559–574, doi: 10.1016/j.jaridenv.2003.11.009.

Wang, P.X., Clemens, S., Beaufort, L., Braconnot, P., Ganssen, G., Jian, Z.M., Kershaw, P., and Sarnthein, M., 2005, Evolution and variability of the Asian monsoon system: State of the art and outstanding issues: Quaternary Science Reviews, v. 24, p. 595–629, doi: 10.1016/j.quascirev.2004.10.002.

Manuscript received 25 June 2008
Revised manuscript received 3 November 2008
Manuscript accepted 6 November 2008

Printed in USA